Analysis of a protein region involved in permeation and gating of the voltage-gated *Torpedo* chloride channel ClC-0

Uwe Ludewig, Thomas J. Jentsch and Michael Pusch *

Centre for Molecular Neurobiology (ZMNH), Hamburg University, Martinistrasse 52, D-20246 Hamburg, Germany

1. The chloride channel from the *Torpedo* electric organ, ClC-0, is controlled by two distinct ('fast' and 'slow') voltage-dependent gates. Here we investigate the effects of mutations in a region after putative transmembrane domain D12. A mutation in this region has previously been shown to change fast gating and permeation.

2. We used a combination of site-directed mutagenesis with two-electrode voltage-clamp and patch-clamp measurements.

3. Most conservative substitutions have minor effects, while more drastic mutations change kinetics and voltage dependence of fast gating, as well as ion selectivity and rectification.

4. While ClC-0 wild-type (WT) channels deactivate fully in two-electrode voltage clamp at negative voltages, channels do not close completely in patch-clamp experiments. Open probability is increased by intracellular chloride in a concentration- but not voltage-dependent manner.

5. In several mutants, including K519R, the minimal macroscopic open probability of fast gating is larger than in WT. Mutant channels fluctuate at negative potentials between open and closed conformations. Open probability is much more effectively increased by intracellular chloride than in WT. The observations support the idea that permeating ions inside the pore stabilize the open state.

6. Besides effects on permeation and gating of single protopores, some mutations affect 'slow' gating. In summary, the region after D12 participates in fast as well as in slow gating; mutations additionally influence permeation properties.

The voltage-dependent chloride channel from *Torpedo* electric organ, ClC-0 (White & Miller, 1979; Miller & Richard, 1990; Jentsch, Steinmeyer & Schwarz, 1990), is the best characterized member of a family of chloride channels or putative chloride channels (Jentsch, Günther, Pusch & Schwappach, 1995). Gating of ClC-0 is voltage dependent with two apparently independent gates working in opposite voltage directions: a 'slow' gate activates the channel at negative membrane voltages and a 'fast' gate opens it at positive voltages (Miller & Richard, 1990). These two gates are easily distinguished at the single-channel level, where ClC-0 displays a characteristic behaviour: opening occurs in bursts, whose durations are determined by the slow gate; within a single burst the channel fluctuates between the closed state and two equally spaced conductance levels in a binomial manner (Miller, 1982). The fluctuations within a burst correspond to the gating transitions of the fast gate. Based on these findings, Miller proposed (Miller, 1982) that the channel is a functional dimer of two identical 'protochannels', which can be closed individually by the fast gate and internal application of the chloride channel blocker 4,4′-diisothiocyanatostilbene-2,2′-disulphonic acid (Miller & White, 1984). This model was confirmed in a co-expression study of mutant and wild-type subunits, where it was shown that each channel consists of two seperate ionic pathways ('protopores') that are individually gated by a fast gating mechanism (Ludewig, Pusch & Jentsch, 1996; Middleton, Pheasant & Miller, 1996). In contrast to fast gating, both protopores are simultaneously opened and closed by a common slow mechanism. The functional properties of this slow gating are determined by the subunits and their interaction (Ludewig *et al.* 1996). Sucrose gradient sedimentation (Middleton, Pheasant & Miller, 1994) and functional analysis (Ludewig *et al.* 1996; Middleton *et al.* 1996) suggest that the double barrelled channel corresponds to a dimer of two subunits. In contrast, Steinmeyer, Lorenz, Pusch, Koch & Jentsch (1994) concluded from functional analysis of ClC-1 channels, a subunit composition of more than two subunits for ClC proteins.

* To whom correspondence should be addressed.

Recently, fast gating was shown to depend strongly on the external anion concentration (Pusch, Ludewig, Rehfeldt & Jentsch, 1995*a*). The open probability (P_o) is shifted to more positive voltages as the concentration of external permeant anions is reduced. We proposed a gating mechanism in which the permeating anion itself is the voltage-sensing charge, whereas the actual opening and closing transitions are intrinsically voltage independent (Pusch *et al.* 1995*a*). This gating model differs fundamentally from the mechanism suggested for a cation channel superfamily. In that case, 'intrinsic' gating charges on the protein, which are located in a transmembrane span (the 'S4' segment), sense the voltage drop over the membrane. Their movement in response to the electric field leads to gating transitions even in the absence of permeation (reviewed by Sigworth, 1994).

The 'extrinsic' gating mechanism of ClC-0 probably applies for other ClC channels as well. Similar to ClC-0 fast gating, ClC-1 channels deactivate at hyperpolarizing potentials when expressed in oocytes (Steinmeyer, Ortland & Jentsch, 1991), in mammalian cells (Pusch, Steinmeyer & Jentsch, 1994) and in insect cells (Astill, Rychkov, Clarke, Hughes, Roberts and Bretag, 1996). Opening of ClC-1 is also facilitated by external chloride (Rychkov, Pusch, Astill, Roberts, Jentsch & Bretag, 1996). Opposite results, however, were reported by Fahlke, Rüdel, Mitrović, Zhou & George (1995). The discrepancy can probably, however, be explained by the use of methane sulphonate to replace chloride by Fahlke *et al.* (1995), an anion that itself has strong effects on gating of ClC-1 (authors' unpublished observation).

Additional support for the extrinsic gating mechanism of ClC-0 came from the properties of a ClC-0 point mutant (K519E). Its gating still depends on the extracellular anion concentration, but is drastically slowed. The ion selectivity and the rectification of the open channel are also changed (Pusch *et al.* 1995*a*). In this mutant the characteristics of single protopores were specifically altered, while the common slow gating process was unaffected. We have now constructed and analysed mutants in the region surrounding K519, which is highly conserved between ClC-0, ClC-1, ClC-2, and ClC-K proteins (Fig. 1*B*; Jentsch *et al.* 1990; Steinmeyer *et al.* 1991; Thiemann, Gründer, Pusch & Jentsch, 1992; Uchida, Sasaki, Furukawa, Hiraoka, Iwai, Hirata & Marumo, 1993; Kieferle, Fong, Bens, Vandewalle & Jentsch, 1994). The present analysis supports and extends our previous conclusion that this region is important for fast gating and permeation and reveals additionally, that some mutations also alter slow gating. Furthermore, we find that gating of protopores is, especially in mutants, influenced by internal chloride.

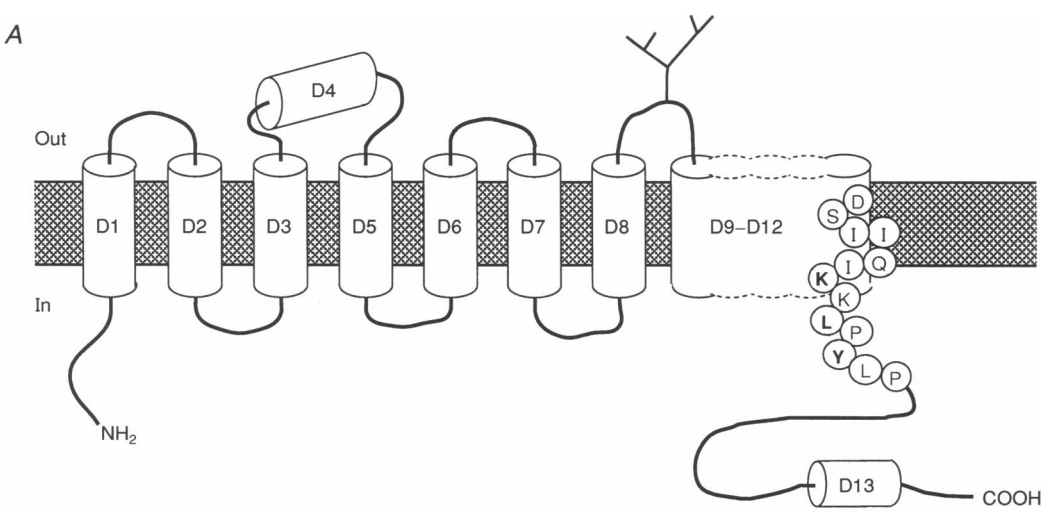

B

CLC-0	--L**YD**SIIQI**KKLPYLP**ELS--
CLC-1	--L**YD**SIIQV**KKLPYLP**DLG--
CLC-2	--L**YD**SIIRI**KKLPYLP**ELG--
CLC-Ka	--F**YD**GTIIV**KKLPYLP**RIL--
CLC-Kb	--F**YD**GTVIV**KKLPYLP**RIL--

Figure 1. Transmembrane topology of ClC-0 channels

A, with the exception of D4 (whose sequence and hydrophobicity is not well conserved in other ClC proteins), the hydrophobic domains D1 to D8 are assumed to cross the membrane once. The topology of the broad hydrophobic region D9–D12 is unknown. It is thought to cross the membrane in an uneven number. Residues 513 to 525 at the end of the putative transmembrane domain D12 were mutated in this study and are explicitly shown. Residues in bold show importance in permeation and fast gating. *B*, sequences from the region surrounding K519 which are highly conserved for ClC-0, ClC-1, ClC-2 and ClC-K proteins. Conserved residues are shown in bold.

METHODS

Mutagenesis and channel expression

Mutations were introduced by recombinant polymerase chain reaction and verified by sequencing. Most mutants were cloned into pBluescript together with the native ClC-0 5′ untranslated region. To boost expression, several mutants were cloned into a vector containing *Xenopus* β-globin untranslated sequences (Krieg & Melton, 1984). The constructs were linearized and capped cRNA was transcribed *in vitro* using T3 (pBluescript constructs) or SP6 RNA polymerase (other constructs) and the mMessage mMachine kit (Ambion, Austin, TX, USA). cRNA was diluted to about 30–100 mg l^{-1} before injection. Ovaries were obtained from frogs that had been anaesthetized with tricaine (0·17%) for 15 min. After surgery, frogs were allowed to recover from anaesthesia and suitable aftercare was given. Stage V and VI *Xenopus* oocytes were then manually defolliculated and injected with 50 nl of cRNA solution. For patch clamping, defolliculated oocytes were collagenase treated (1 g l^{-1} Sigma Type II for 10–15 min) before injection, and the vitelline membrane was removed manually after incubation of oocytes in hypertonic medium directly before the experiment (Methfessel, Witzemann, Takahashi, Mishina, Numa & Sakmann, 1986). Oocytes were kept in Barth's solution at 14–19 °C.

Electrophysiology and data analysis

Currents were measured at room temperature (22 ± 2 °C) 1–3 days after injection using two-electrode voltage clamp and pCLAMP 5·5 software. Microelectrodes were filled with 3 M KCl and had resistances of 0·3–0·6 MΩ. Leakage or capacitative currents were not subtracted. Capacitative transients were cut off in some figures for clarity. In all figures zero current is indicated by dashed lines. Mutants were routinely measured in at least two batches of oocytes. To study the fast gate and the permeation properties, the slow gate was maximally opened by hyperpolarizing prepulses. Since the slow gating closes the channel only very slowly, compared with the gating relaxations of the fast gate, the slow gate remains open during such experiments. A typical voltage protocol is shown in Fig. 4*A*. Fast gates were maximally opened by a short prepulse to +60 mV, then a different test pulse was applied in each run. The instantaneous *I–V* relation was determined by fitting a mono-exponential function to the currents at the test pulse and by extrapolating it to its beginning. The open probability of the fast gate ($P_{o,fast}$) was determined at −100 mV after various test potentials (Pusch *et al.* 1995*a*). At this potential, relaxations were sufficiently slow when compared with capacitative transients to reliably extrapolate currents to the onset of the pulse. Currents thus obtained were then normalized to the maximum current flowing after positive prepotentials to yield the apparent $P_{o,fast}$. Similar values for $P_{o,fast}$ are obtained when steady-state currents are divided by instantaneous currents right after the prepulse (Fig. 3). Apparent $P_{o,fast} = f(V)$ was fitted with a Boltzmann distribution containing a variable offset P_{min}. This yields the half-maximal activation voltage $V_{½,fast}$ and the nominal gating charge z_n:

$$P_{o,fast} = P_{min} + (1 - P_{min})/(1 + \exp(z_n e_o(V_{½,fast} - V)/kT)),$$

with the elementary charge e_o, the voltage V, the Boltzmann constant k and the absolute temperature T. We used the SigmaPlot program (Jandel Scientific, Corte Madera, CA, USA) for fitting.

Currents were recorded in ND96 solution composition (mM): NaCl, 96; KCl, 2; $CaCl_2$, 1·8; $MgCl_2$, 1; Hepes, 5; pH 7·4, total calculated chloride concentration: 103·6 mM or in solutions in which 80 mM Cl^- was replaced by Br^-, I^-, NO_3^- or glutamate$^-$ (leaving 23·6 mM chloride). Permeability coefficients P_x were calculated from reversal potential measurements in biionic conditions using the following equation (Goldman–Hodgkin–Katz equation; Hille, 1992):

$$P_x = (103{\cdot}6\exp(e_o(V_{rev,ND96} - V_{rev,x})/kT) - 23{\cdot}6)/80,$$

where $V_{rev,ND96}$ is the reversal potential in ND96, $V_{rev,x}$ is the reversal potential with 80 mM chloride replaced by another anion, and k, e_o, and T have their usual meanings.

For cell-attached patch recording (Hamill, Marty, Neher, Sakmann & Sigworth, 1981), oocytes were bathed in solution of composition (mM): *N*-methyl-D-glucamine-chloride (NMDG-Cl), 100; $CaCl_2$, 1·8; Na-Hepes, 5; at pH 7·4. For inside-out patch recording oocytes were bathed in 100 mM NMDG-Cl solutions, with (mM): $MgCl_2$, 2; Na-Hepes, 5; EGTA, 5; pH 7·4, or solutions in which NMDG-Cl was partially replaced by NMDG-glutamate. Pipettes were filled with a solution of composition (mM): NMDG-Cl, 100; $CaCl_2$, 1·8; Na-Hepes, 5; pH 7·4. Macroscopic data were low-pass filtered at 5 kHz. Single-channel data were filtered at 1 kHz.

Steady-state activation of the slow gate was studied with a protocol containing prepulses of 6 s duration from +60 to −140 mV in steps of 20 mV. Channel activation was then monitored directly after each pulse at a constant potential of +40 mV. A single Boltzmann distribution with a variable offset was sufficient to describe the steady state of slow gating. Deactivation of the slow gate was monitored by repetitive short pulses to +40 mV while holding the oocyte at its reversal potential.

RESULTS

Effects of mutations on permeation and fast gating

Fast gating of WT ClC-0 can be studied independently from slow gating because the slow gate stays open for minutes once it has been opened by hyperpolarization (Pusch *et al.* 1995*a*). Typical current traces from wild-type (WT) ClC-0 are shown in Fig. 2*A* (left panel). After opening the fast gate by an additional depolarizing prepulse, channels deactivate at negative voltages with a single-exponential time course and a maximum time constant of ~10 ms at −100 mV. Activation and deactivation relaxations have similar time courses. Time constants obtained from mono-exponential fits show a bell-shaped voltage dependence (Fig. 2*C*). Apparent $P_{o,fast}$ is well described by a single Boltzmann distribution with an apparent gating valence of 0·93 (Fig. 3, Table 1). Single-channel studies (Miller, 1982; Hanke & Miller, 1983) indicate that channels are fully open at saturating positive potentials, suggesting that macroscopic (normalized) apparent $P_{o,fast}$ reflects the true open probability of the fast gate of WT ClC-0.

In a previous study (Pusch *et al.* 1995*a*) a lysine at position K519 was identified that is important for fast gating and pore properties. Replacements of lysine 519 by glutamine, glutamate or histidine all resulted in similar currents (Table 1, Pusch *et al.* 1995*a*). When the positive charge was conserved (K519R), however, the phenotype was intermediate to WT. Macroscopic currents for this mutant are shown in Fig. 2*A*. Mutant K519R displays slower kinetics and a slight outward rectification. In addition, steady-state

currents do not vanish at negative voltages. The resulting apparent $P_{o,fast}$ approaches a minimal value of ~10% at the most negative voltages (Fig. 3). As expected by the predicted localization of K519 close to the cytoplasmic side, fast gating and permeation in mutant K519H were not sensitive to external pH changes (between 6·2 and 9·0, data not shown). As K519 is located in a conserved stretch of amino acids (Fig. 1*B*) we sought to investigate the effects of point mutations of neighbouring residues (Table 1).

Most substitutions amino-terminal to K519 (mostly conservative exchanges) did not significantly change ClC-0 in its permeation and fast gating properties. The only exceptions were Q517R, which had a slightly increased Br^- permeability, and D513N, for which no functional expression could be obtained.

Mutants at residue 520 had WT characteristics. In contrast, several substitutions carboxy terminal to it changed channel characteristics. Conservative exchanges at positions 521 and 522 resulted in a slight outward rectification (Table 1, Fig. 2), and channels which had L521 or Y523 replaced by lysine resembled the protopore properties of K519 mutants: currents were outwardly rectifying, gating kinetics were slower and the voltage dependence of $P_{o,fast}$ was shifted to more positive potentials (Figs 2 and 3). In addition, again resembling K519 mutants, apparent minimal $P_{o,fast}$ saturated at a value that was significantly larger than zero (Fig. 3).

Smaller offsets in the apparent $P_{o,fast}$ were seen with L521I, as well as in mutants at position 522. Since substitutions at position 522 had drastic effects on slow gating kinetics, fast gating parameters could not be determined reliably, as explained later (Effects of mutations on slow gating).

K519E mutant channels are less selective among halide ions than WT ClC-0 (Pusch *et al.* 1995*a*). In contrast to WT, Br^- and Cl^- conduct equally well at positive potentials and I^- conductance is increased (Pusch *et al.* 1995*a*). If selectivity is assessed by permeability coefficients (Table 1), however, the

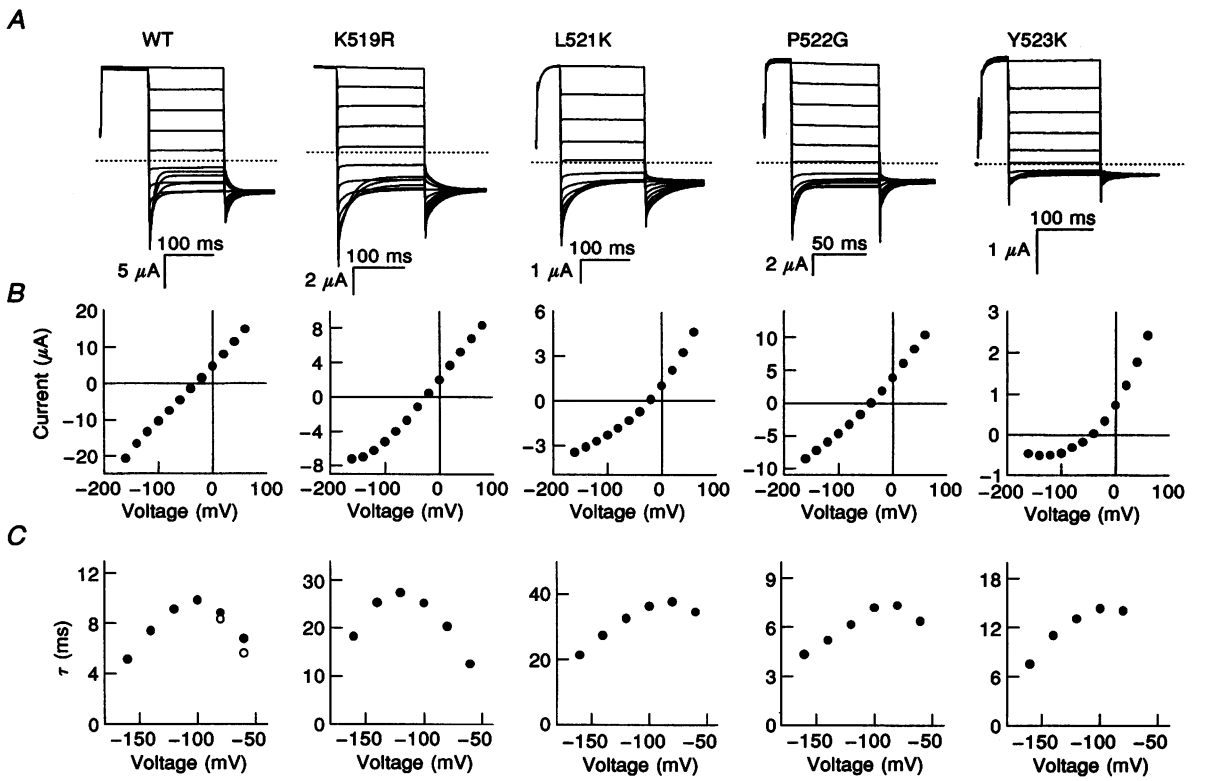

Figure 2. Electrophysiological characteristics of ClC-0 wild-type and K519R, L521K, P522G and Y523K mutant channels

A, representative voltage-clamp traces in ND96. After opening the 'slow' gate by hyperpolarization and a step to +60 mV to open 'fast' gates, voltage pulses from +80 to −160 mV were applied in 20 mV steps and followed by a constant pulse to −100 mV. The voltage protocol is also shown in Fig. 4*A*. Currents from K519R, L521K and Y523K are outwardly rectifying and have slower kinetics than WT. In some recordings, capacitative transients have been blanked out for clarity. *B*, instantaneous *I–V* relations from the traces shown in *A*. *C*, time constants of deactivation deduced from traces in *A* (●). Activation time constants from the same experiment at −60 and −80 mV are also shown for WT (○). Activating and deactivating currents had similar relaxation times at all voltages where both could be measured (i.e. −120 to −60 mV in regular chloride). Note the different time scales and current magnitudes for the mutants. Dashed lines, here and in following figures, indicates zero current.

Table 1. Conduction and gating properties of the mutants investigated

Mutant	IV	τ_{max} (ms)	$V_{½,fast}$ (mV)	z_{fast}	Offset (%)	P_{Br}/P_{Cl}	P_I/P_{Cl}	P_{NO_3}/P_{Cl}	$V_{½,slow}$ (mV)	z_{slow}	τ_{slow} (s)
WT	Lin.	10	−86±18	0·93±0·15	<5(12)	0·67±0·05(10)	0·19±0·04(10)	0·62±0·09(6)	−95±11(13)	2·2±0·2	411±207(18)
D513E	Lin.	10	−83±7	0·80±0·04	<5(3)	0·65±0·14(4)	0·22±0·07(3)	n.d.	−89±8(3)	2·0±0·1	51±35(3)
S514A	Lin.	10	−90±10	0·98±0·01	<5(5)	0·64±0·17(4)	0·26±0·08(4)	0·60±0·08(2)	−75±2(5)*	2·3±0·2*	>200(1)
I515L	Lin.	10	−87±19	0·92±0·08	<5(3)	0·73±0·08(4)	0·21±0·11(3)	n.d.	−84±8(4)	2·3±0·8	>200(1)
I516L	Lin.	10	−89±15	0·90±0·17	<5(5)	0·68±0·02(2)	0·21±0·12(2)	n.d.	−93±10(5)	2·0±0·4	85±53(3)
Q517R	Lin.	10	−90±21	0·90±0·11	<5(7)	**0·82±0·10(5)**	0·23±0·03(3)	n.d.	−93±8(5)	2·3±0·7	122±40(3)
I518L	Lin.	10	−82±12	0·81±0·06	<5(6)	0·76±0·06(2)	0·27±0·03(2)	0·61(1)	−101±12(3)	2·4±0·3	300(1)
K519R	**SOR**	**15**	−83±22	0·78±0·02	**10±7(3)**	0·66±0·04(3)	0·19±0·03(2)	0·63±0·08(2)	−83±3(3)	2·5±0·7	566±613(2)
K519H	**OR**	**30**	**−66±14**	0·77±0·06	**14±2(4)**	**0·81±0·05(3)**	0·24±0·03(3)	0·55±0·02(3)	−88±1(3)	2·1±0·3	n.d.
K519Q	**OR**	**70**	**−70±13**	0·63±0·10	**41±5(4)**	**0·82±0·03(6)**	0·11±0·05(6)	n.d.	−87±5(2)	2·2±0·2	>200
K519E	**OR**	**70**	**−73±13**	0·70±0·04	**34±4(9)**	**0·82±0·04(8)**	0·24±0·06(6)	0·61±0·14(3)	−104±9(5)	2·0±0·2	970±200(2)
K520Q	Lin.	10	−86±13	0·91±0·07	<5(5)	0·66±0·03(3)	0·17±0·08(3)	0·58(1)	−96±2(2)	2·4±0·3	223(1)
K520E	Lin.	10	−93±9	0·92±0·03	<5(3)	0·72±0·05(5)	0·20±0·08(4)	0·58(1)	−106±4(4)	1·8±0·1	420±154(3)
L521I	**SOR**	10	−77±2	0·67±0·10	**14±4(6)**	**0·79±0·02(5)**	0·22±0·10(5)	0·63±0·03(2)	−77±5(6)	1·9±0·3	**11±8(6)**
L521K	**OR**	**45**	**−67±13**	0·83±0·10	**28±6(3)**	**0·82±0·06(4)**	0·21±0·06(4)	0·69±0·11(4)	−82±3(4)	2·2±0·1	**28±1(2)**
P522G	**SOR**	10	**−69±15**	0·84±0·12	13±13(4)	0·72±0·06(4)	0·23±0·10(4)	0·66±0·11(2)	−82±6(6)	2·0±0·1	**14±11(7)**
P522L	**SOR**	*	*	*	*	0·70±0·11(6)	0·29±0·09(5)	0·65±0·18(5)	−62±10(4)*	1·5±0·2*	**10±1(2)**
P522K	**SOR**	*	*	*	*	0·75±0·06(5)	0·25±0·02(5)	0·65±0·02(5)	−94±13(5)	2·3±0·4	**4±2(3)**
Y523F	Lin.	10	−87±14	0·83±0.13	<5(5)	0·68±0·07(2)	0·16±0·03(3)	0·53(1)	−82±6(3)	2·0±0·3	89±23(3)
Y523K	**OR**	**15**	**−48±21**	0·81±0·12	**34±11(4)**	0·69±0·07(5)	0·26±0·07(3)	0·59±0·10(5)	−87±12(8)	2·1±0·4	**14±5(3)**
L524I	Lin.	10	−84±21	0·88±0·06	<5(4)	0·71±0·11(3)	0·22±0·07(2)	0·64±0·09(2)	−78±8(7)	2·2±0·5	>1000(4)
P525G	Lin.	10	−95±12	0·87±0·16	<5(4)	0·70±0·05(2)	0·21±0·14(3)	0·63±0·12(2)	−66±9(3)*	1·8±0·2*	>200(3)

In general, only relative conservative exchanges were made. For those positions where conservative substitutions had interesting effects on permeation or gating, more drastic exchanges were introduced. Permeation coefficients were obtained as explained in Methods. Open probability of the fast and slow gate were obtained as described in Methods and fitted with a simple Boltzmann function. In some mutants, values could not be determined reliably and are therefore marked by *. The similar time course of both gates at negative voltages in P522L and P522K made it impossible to measure steady-state $P_{o,fast}$ reliably. In mutants P522L and P525G $P_{o,slow}$ deviates from a simple Boltzmann distribution. For those mutants a Boltzmann function was fitted to the $P_{o,slow}$ at voltages more positive than −100 mV, where $P_{o,slow}$ could be described by a Boltzmann function. In mutants S514A and L524I only a relatively small amount of current could be further activated by hyperpolarizing prepulses. There is some variability in the steady-state parameters of fast and slow gating for each mutant even in oocytes from the same frog. The variability of $V_{½,fast}$ may be due to differences in internal pH of different oocytes to which ClC-0 gating is very sensitive (Hanke & Miller, 1983). The apparent variability in selectivity may be due to variable expression of endogenous anion selective oocyte channels. Bold values are significantly different from the corresponding WT phenotype. (Lin., linear; OR, outwardly rectifying; SOR, slightly outwardly rectifying; n.d., not determined; numbers of independent experiments are given in brackets).

difference between WT and K519E is rather small. A similar effect on halide selectivity was observed also with L521K and Y523K mutants; the overall permeability sequence of $Cl^- > Br^- \approx NO_3^- > I^-$ > glutamate$^-$, however, was not changed by any mutation (Table 1). Similar to wild-type (Pusch *et al.* 1995*a*), the open probability of all mutants is shifted to more positive values with less external permeant anions (data not shown).

Fast gating of WT channels is sensitive to variations of internal chloride

The intracellular chloride concentration of oocytes is about 30 mM, a value that can be calculated from reversal potential measurements. With this intracellular chloride concentration the minimal open probability at negative potentials of wild-type approaches zero in two-electrode voltage-clamp experiments (Figs 3 and 4*B*). In cell-attached patches on oocytes, however, the minimal open probability saturates at a non-zero value (Fig. 4*C*). We have no final explanation for this discrepancy of the results obtained by the two different methods. Differences may be due to depletion of chloride at the inner surface of oocyte membranes during two-electrode voltage-clamp experiments or due to clamp problems ('space clamp', Stühmer, 1992).

In order to investigate in more detail a possible dependence of the minimal open probability on the intracellular chloride concentration we performed patch-clamp experiments on

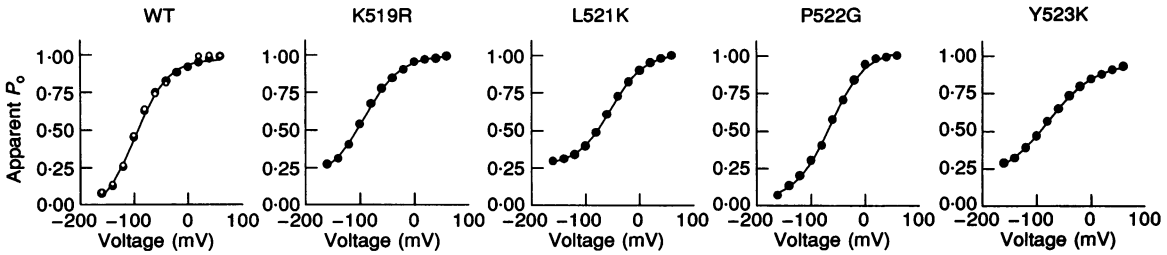

Figure 3. Apparent open probability of ClC-0 wild-type and mutants K519R, L521K, P522G and Y523K

Macroscopic $P_{o,fast}$ obtained from traces in Fig. 2 at a constant test pulse to −100 mV after various pre-potentials (●). For WT the apparent $P_{o,fast}$ deduced by dividing steady state by instantaneous currents from the same record is also shown (○). At voltages near the reversal (namely 0 and −20 mV) instantaneous and steady-state currents are very small leading to large error when the ratio is calculated. Values at these voltages are therefore not included in the figure. Because of this uncertainty of determing $P_{o,fast}$ at voltages near the reversal when calculated by this method, $P_{o,fast}$ was generally deduced from the more reliable method explained in Methods. Note that apparent $P_{o,fast}$ saturates at a non-zero value in mutants K519R, L521K and Y523K. Continuous lines represent Boltzmann distributions as detailed in Methods. For steady-state activation parameters of mutants see Table 1.

WT ClC-0 in the inside-out configuration (Fig. 5). Similar to measurements in the cell-attached configuration, the minimal apparent $P_{o,fast}$ is clearly larger than zero at all concentrations tested (Fig. 5*B*). The minimal macroscopic $P_{o,fast}$ is about 30% in high (104 and 64 mM) intracellular chloride. It becomes slightly smaller in intermediate (24 mM) chloride. At the lowest concentration that still allowed a reliable measurement of inward currents (4 mM) the minimal $P_{o,fast}$ is decreased even further to ~11% (Fig. 5*B*), while neither the slope nor the half-maximal voltage of activation is changed (see also Pusch *et al.* 1995*a*).

While the low single-channel current and fast gating kinetics prohibited the reliable measurement of the $P_{o,fast}$ of single ClC-0 WT channels at negative voltages in low intracellular chloride, $P_{o,fast}$ of single channels was determined for high intracellular chloride. Open probabilities of single ClC-0 WT channels at various voltages are shown in Fig. 5*B* (filled circles). Measurements of single-channel $P_{o,fast}$ are not influenced by leak currents. This explains the observation that the macroscopic estimates are slightly larger than the values obtained from single channels. Even at the most negative potentials, however, the single-channel open probability saturates at a value of about 20%. In addition to effects on the $P_{o,fast}$, higher intracellular chloride concentrations slightly increase the time constants of deactivation (Fig. 5*C*).

In summary, we observe a different behaviour of the fast gate of WT ClC-0 at negative voltages when measured with two-electrode voltage clamp compared with patch clamp. Whereas two-electrode voltage-clamp measurements suggest

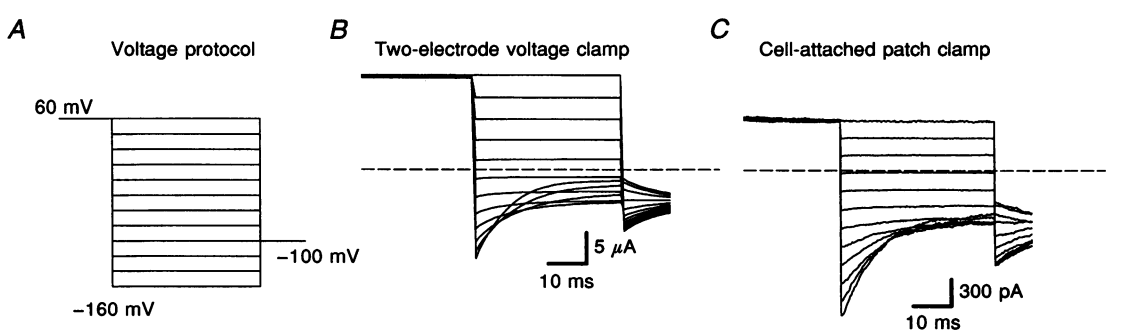

Figure 4. Comparison of two-electrode voltage-clamp measurements with patch-clamp measurements of ClC-0 WT channels in oocytes

A, voltage protocol; *B*, family of macroscopic currents measured from a whole oocyte with two-electrode voltage clamp. Currents elicited by the voltage protocol in *A*. *C*, macroscopic currents measured in the cell-attached configuration of the patch-clamp technique.

that WT channels deactivate completely at negative voltages, channels have a significant open probability in patch-clamp experiments. The minimal $P_{o,fast}$ is dependent on internal chloride being decreased at lower concentrations. The reason for complete deactivation in two-electrode voltage-clamp measurements remains to be resolved.

Mutant K519R channels are strongly activated by intracellular chloride

The minimal apparent $P_{o,fast}$ of several outwardly rectifying mutants saturates at a non-zero value at hyperpolarizing voltages (Fig. 3, Table 1), even when measured with the two-electrode voltage clamp. This residual $P_{o,fast}$ was independent of the expression level, ruling out the possibility that endogenous oocyte currents significantly contribute to this offset. At negative voltages, this leads to a residual steady-state current component. The channels carrying this current could be closed by the slow gating mechanism (data not shown).

In inside-out patch experiments with 24 mM intracellular chloride, the mutant K519R has a steady-state open probability similar to wild-type (Fig. 6*B*). The minimal $P_{o,fast}$ saturates at a non-zero value, in the case of K519R approximately in accordance with whole-cell two-electrode measurements (Fig. 3). As also observed in wild-type, intracellular chloride increases $P_{o,fast}$, but much more drastically than in WT: at 104 mM internal chloride, channels are more than 50% open even at the most negative potentials (Fig. 6*A* and *B*). This increase of $P_{o,fast}$ by intracellular chloride is consistent with the assumption that permeant ions inside the pore influence open probability of protochannels. The voltage-dependent parameters of $P_{o,fast}$ are unaffected by internal chloride (not shown, see also Pusch *et al.* 1995*a*). Thus the rise in $P_{o,fast}$ by intracellular chloride is largely voltage independent.

In order to investigate in more detail the mechanism that leads to the large steady-state inward currents at negative

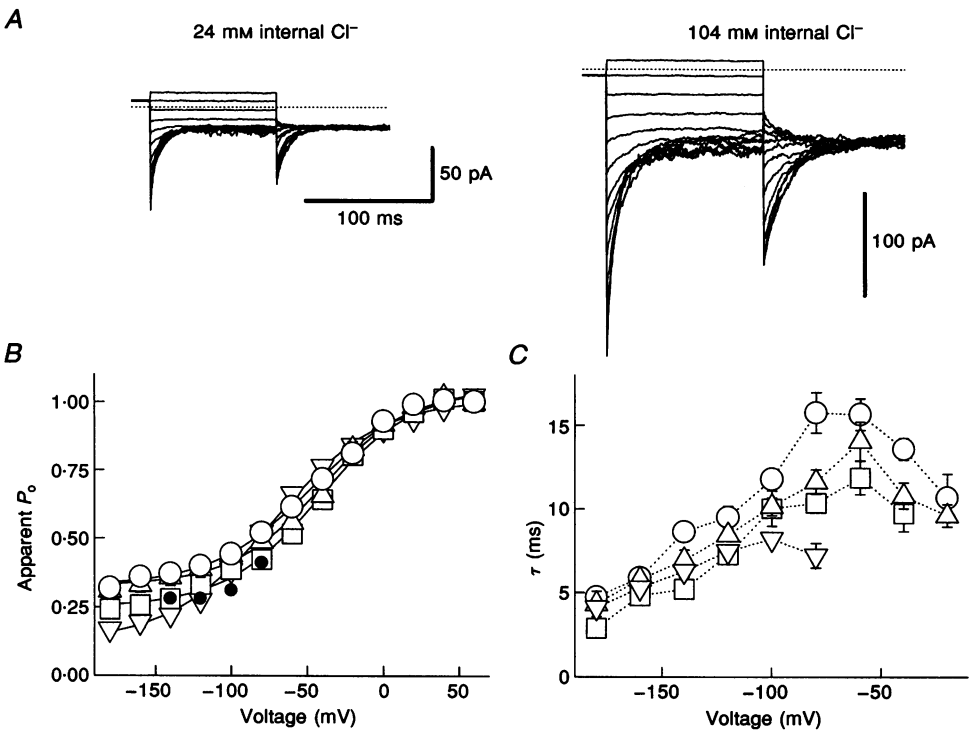

Figure 5. Patch-clamp measurements of ClC-0 WT channels in various internal chloride concentrations

A, family of macroscopic currents obtained by stepping the membrane potential from 60 to −160 mV in 20 mV steps followed by a constant tail potential of −100 mV in 24 mM internal chloride (left) and 104 mM internal chloride (right) from the same inside-out patch. *B*, macroscopic $P_{o,fast}$ in different internal chloride concentrations obtained from 6 independent measurements as shown in *A*, ▽, 4 mM; □, 24 mM chloride; △, 64 mM; ○, 104 mM chloride. Note the different minimal $P_{o,fast}$ at negative voltages for different internal chloride concentrations. $P_{o,fast}$ values at −140 mV in 64 mM chloride are not statistically different from values in 104 mM, but $P_{o,fast}$ in 24 mM ($P < 0{\cdot}05$) and 4 mM ($P < 0{\cdot}001$) is significantly different from that in 104 mM (Student's *t* test). Since some current in patch recordings may be due to unspecific leak conductance, a small percentage of the total current is probably carried by a leak conductance. ●, open probability directly obtained from single-channel measurements. *C*, time constants of deactivation in different internal chloride concentrations. Symbols as in *B*.

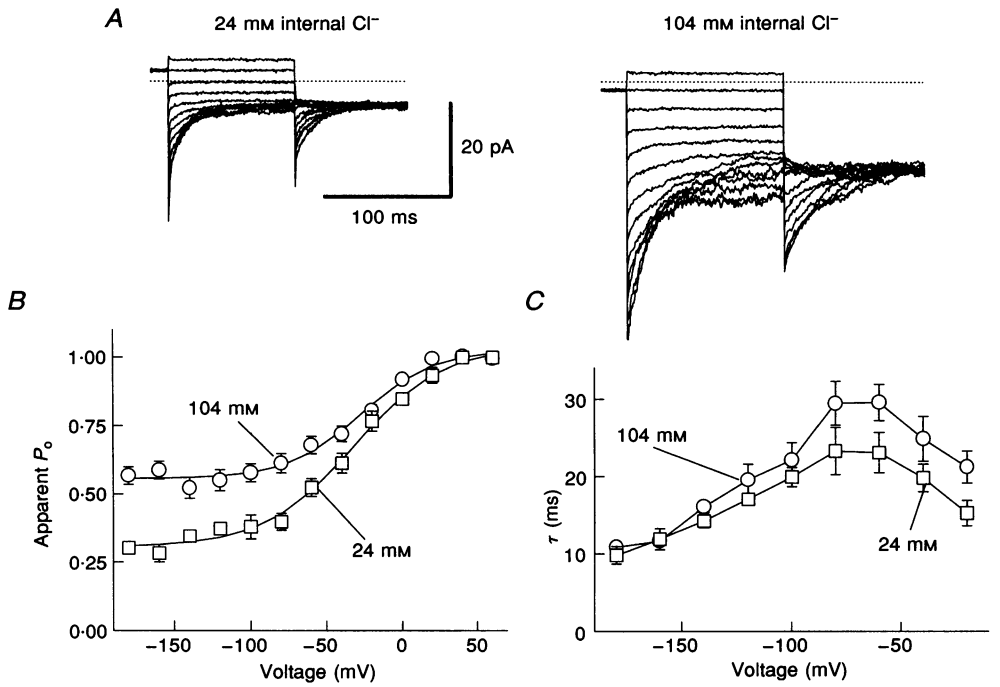

Figure 6. Patch-clamp measurements of K519R mutant channels in different internal chloride concentrations

A, family of macroscopic currents obtained by stepping the membrane potential from 60 to −160 mV in 20 mV steps followed by a constant tail potential of −100 mV in 24 mM internal chloride (left) and 104 mM internal chloride (right) from the same inside-out patch. *B*, macroscopic $P_{o,fast}$ in different internal chloride concentrations obtained from 4 independent measurements as shown in *A*. □, 24 mM chloride; ○, 104 mM chloride. *C*, time constants of deactivation in different internal chloride concentrations. Symbols as in *B*.

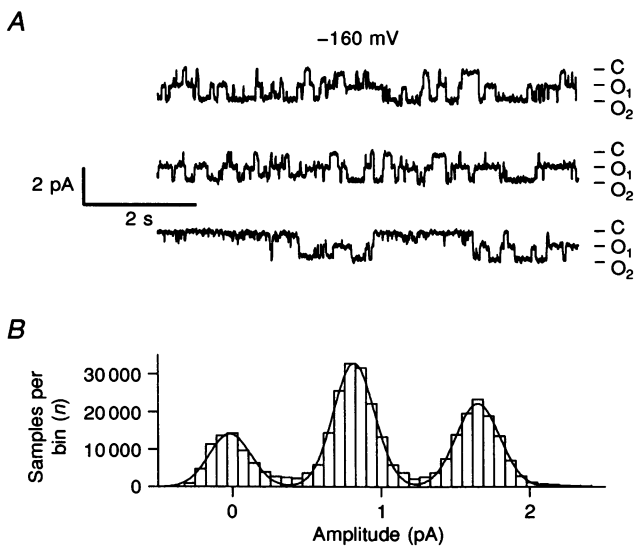

Figure 7. Channels do not fully deactivate at negative potentials and fluctuate between open and closed conformations

A, single-channel trace of K519R mutant at −160 mV in 104 mM internal chloride. The double-barrelled channels fluctuate between 3 conductance levels: zero (C) 6 pS (O_1) and 12 pS (O_2). *B*, amplitude histogram from a burst of openings (where the slow gate has activated a single channel) in the same conditions as in *A* reveals an open probability of 56% at −160 mV. Similar results were obtained in an additional single-channel experiment and confirmed by several experiments using noise analysis of hundreds of channels.

potentials, we measured single mutant K519R channels. In Fig. 7*A* a recording of a single mutant channel at −160 mV is shown. The mutant displays the typical double-barrelled behaviour. It has, compared with wild-type, a slightly reduced single-channel conductance of ~6 pS. At −160 mV it still fluctuates between the open and closed states. It has an open probability of 56% (Fig. 7*B*), which is voltage independent in this range. This corresponds exactly to the value inferred from the macropatch recordings in the same solutions (Fig. 6). Thus apparent $P_{o,fast}$ matches the absolute single-channel $P_{o,fast}$. Interestingly, the time constants of deactivation decrease with negative voltages down to −160 mV (Fig. 6*C*), where the apparent $P_{o,fast}$ has been practically saturated for both WT and mutants (Figs 5*C* and 6*C*). This implies that both open and closing rates increase proportionally with negative voltage, resulting in a constant ratio (see also Hanke & Miller, 1983; Bauer, Steinmeyer, Schwarz & Jentsch, 1991 for single-channel opening and closing rates).

Effects of mutations on slow gating

To investigate whether mutations in this region specifically affect fast gating and permeation, we also studied their effect on slow gating. Steady-state open probability of slow gating is well described by a simple Boltzmann distribution, and the voltage $V_{½,slow}$ for half-maximal voltage-dependent activation is similar to the $V_{½,fast}$ of the fast gate. However, slow and fast gating have opposite voltage dependencies, and $P_{o,slow}$ depends more strongly on voltage with a nominal gating charge of 2·2 (Fig. 8*B*; Table 1).

Steady-state parameters of the voltage dependency of slow gating are relatively unaffected by mutations in the region under study (Table 1). There is no drastic change in the nominal gating charge and shifts in $V_{½,slow}$ are less then 20 mV.

Several mutations, however, affect the kinetics of slow gating. Gating is at least fivefold faster than WT in mutants I516L and D513E. Kinetics are even faster with mutations at positions L521, P522 and Y523. Kinetics of L521I inactivation at positive potentials are shown in Fig. 8*A* in comparison to WT. There was no simple correlation with effects on permeation or fast gating. In mutant P522K, slow gating is about 100-fold faster than in WT ClC-0. With mutants at position 522, time constants of 'slow' gating come close to those of the 'fast' gate at negative voltages. Therefore, at negative voltages, it was difficult to separate these gating processes.

For mutants P522L and P525G, $P_{o,slow}$ deviated from a simple Boltzmann distribution. As with WT ClC-0, $P_{o,slow}$ increased with hyperpolarizing voltages, but then decreased again at more negative voltages. This non-monotonic behaviour may reflect an additional gating mechanism which closes the channel with strong hyperpolarization. A similar process has been observed in chimeric ClC constructs

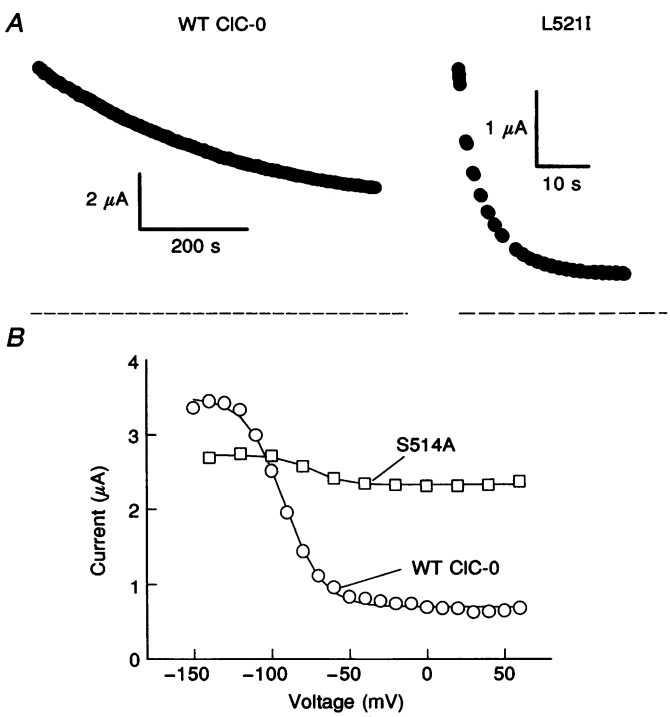

Figure 8. Slow gating is altered in mutants L521I and S514A

A, time course of deactivation in WT ClC-0 (left) and mutant L521I (right) at positive voltages. In these experiments time constants of deactivation were 360 s and 5 s, respectively. *B*, steady-state activation of the slow gate as a function of 7 s prepulses of WT ClC-0 (○) and mutant S514A (□).

(Fong & Jentsch, 1996); here, it was not investigated in more detail. The appearance of this additional gating mechanism interferes with an exact determination of slow gating parameters at hyperpolarizing voltages by shifting the apparent half-maximal voltage $V_{½,slow}$ to more positive potentials, as is observed with P522L and P525G. In addition, the slight decrease in z_{slow} with P522L and P525G (Table 1) may be explained by this effect.

The fraction of current that could be activated by hyperpolarizing pulses relative to the absolute current was slightly variable in different oocytes; in mutants S514A and L524I this fraction was consistently smaller than in WT ClC-0. As an example the $P_{o,slow}$, a typical steady-state activation of mutant S514A is shown in Fig. 8*A*. Compared with WT, a much smaller fraction of channels can be activated by hyperpolarizing prepulses.

DISCUSSION

In this study we show that several point mutations in the region surrounding K519 (bold residues in Fig. 1*A*) result in a similar phenotype with outward rectification, increased Br^- and I^- conductivity and changed fast gating. The changes in selectivity and single-channel conductance point to a location of at least some mutated residues close to the conduction pathway. The effects of mutations on the current–voltage relation, on internal chloride sensitivity of gating, but similar sensitivity to external chloride is consistent with the interpretation that the region under focus contributes to the inner mouth of the ion selective pore. The residues, however, do not contribute critically to the selectivity filter in ClC-0, as the overall permeability sequence $Cl^- > Br^- \approx NO_3^- > I^- >$ glutamate$^-$ is not changed by any mutant.

In all mutants, fast gating was still dependent on the extracellular anion concentration. In addition, we show in this study that in several mutants the open conformation of protopores is stabilized by intracellular chloride. Recent experiments suggest that external permeant ions have to cross most of the ion selective pore (and the voltage drop across the membrane) to reach their binding site to open the channel (Pusch *et al.* 1995*a*). In accordance with this, internal chloride increases $P_{o,fast}$ relatively voltage independently, since its binding site is located almost at the cytoplasmic face of the channel. If the rate-limiting energy barrier for ion transport is not the innermost barrier, one might expect that intracellular chloride ions then activate gating of protochannels. Thus, these results are in full agreement with our previous conclusion (Pusch *et al.* 1995*a*) that gating and permeation are tightly coupled in ClC-0, and that the gating charge may be the permeating anion itself.

For WT ClC-0, different methods of measurement give slightly different results. When explored by patch recording, the minimal open probability saturates at a non-zero value at negative potentials, in contrast to two-electrode voltage-clamp experiments. One might speculate that the complete deactivation seen in two-electrode voltage-clamp recordings is due to a depletion of chloride at the internal face of the membrane. In inside-out patches such a depletion could be less of a problem because membrane foldings (microvilli) that could impede diffusional equilibration are expected to be 'stretched out' to a sufficient degree during seal formation, though there is no evidence that supports such an idea.

Several mutants show an incomplete deactivation even in two-electrode voltage-clamp measurements. Patch-clamp experiments showed that these mutant channels fluctuate between open and closed states even at the most negative voltages, though gating kinetics become faster, implying that both opening and closing rates increase at negative voltages. The increased minimal $P_{o,fast}$ of the mutants is probably linked to the different sensitivity to internal chloride. Whereas for WT minimal $P_{o,fast}$ saturates at 25–30% with high internal chloride, this value reaches almost 60% for mutant K519R at 104 mM. This difference in sensitivity to internal chloride of mutations at position 519 again supports the proposed cytoplasmic location of the amino acids around K519 (Pusch *et al.* 1995*a*).

Interestingly, the altered fast gating properties in mutants (gating kinetics and increased minimal open probability) correlate with changed open channel rectification and reduced selectivity. The altered pore properties will lead to different ion occupancy in the mutants. If one assumes that ions directly inside the pore affect the gating of single protopores, one may expect differences in fast gating due to changed ion transport rates. Model calculations (authors' unpublished observation) show that the effect of mutations on permeation (and, therefore, ion transport rates) can secondarily lead to changed gating of single protochannels; altered gating kinetics and $P_{o,fast}$ may be explained exclusively by altered pore occupancy of permeant ions.

We have shown that substitution of lysine at position 519 by glutamate has a very similar 'protopore phenotype' as e.g. the substitution of tyrosine at position 523 by lysine. The very similar effect of putative negatively and positively charged residues at neighbouring positions excludes simple electrostatic effects of amino acids in this region. It suggests that not only does the charge of the side-chain influence channel characteristics, but additional properties of the amino acid influences the protopore phenotype.

Mutants at position K519 specifically affect protopore characteristics. In contrast, mutations at several neighbouring residues additionally change the slow gating that operates on both protopores simultaneously. While several mutants display altered slow-gating kinetics, the nominal gating charge and half-maximal voltage $V_{½,slow}$ of $P_{o,slow}$, in contrast, were almost unchanged. Drastic changes in slow-gating kinetics are characteristic for mutations at positions 521–523. There is no simple correlation with the nature of

the substituted residue; some more conservative changes lead to faster 'slow' gating than more drastic ones (L521I *versus* L521K, see Table 1). It appears that the protein region under focus participates in both gating processes, since several mutations affect fast as well as slow gating. This is different from e.g. voltage-gated potassium channels, where distinct protein regions control permeation, activation and N-type inactivation. The fact that mutations of every second amino acid have similar effects on protopore characteristics is compatible with a β-sheet structure of this segment.

A combined effect on fast and slow gating was also observed in mutant S123T, which is located in the region between putative transmembrane domains D2 and D3 (Ludewig *et al.* 1996). Protopore properties were very similar to several mutants described here, and slow gating was almost voltage independent.

Except for structures involved in voltage and volume activation of ClC-2 (Gründer, Thiemann, Pusch & Jentsch, 1992), and effects of ClC-1 mutations found in myotonia congenita (Steinmeyer *et al.* 1994; Fahlke *et al.* 1995; Pusch, Steinmeyer, Koch & Jentsch, 1995*b*), little is known about structure–function relationship of other ClC chloride channels. The present results will help in understanding the mechanisms of gating and conduction in those channels.

Astill, D. St J., Rychkov, G. Y., Clarke, J. D., Hughes, B. P., Roberts, M. L. & Bretag, A. H. (1996). Characteristics of skeletal muscle chloride channel ClC-1 and point mutant R304E expressed in Sf-9 cells. *Biochimica et Biophysica Acta* **1280**, 178–186.

Bauer, C. K., Steinmeyer, K., Schwarz, J. R. & Jentsch, T. J. (1991). Completely functional double-barrelled chloride channels expressed from a single *Torpedo* cDNA. *Proceedings of the National Academy of Sciences of the USA* **88**, 11052–11056.

Fahlke, C., Rüdel, R., Mitrović, N., Zhou, M. & George A. L. Jr, (1995). An aspartic acid residue important for voltage-dependent gating of human muscle chloride channels. *Neuron* **15**, 463–472.

Fong, P. & Jentsch, T. J. (1996). Elimination of ClC-0 slow gating. *Biophysical Journal* **70**, A8.

Gründer, S., Thiemann, A., Pusch, M. & Jentsch, T. J. (1992). Regions involved in the opening of ClC-2 chloride channel by voltage and cell volume. *Nature* **360**, 759–762

Hamill, O. P., Marty, A., Neher, E., Sakmann, B. & Sigworth, F. J. (1981). Improved patch clamp techniques for high-resolution current recording from cells and cell-free membrane patches. *Pflügers Archiv* **391**, 85–100.

Hanke, W. & Miller, C. (1983). Single chloride channels from *Torpedo* electroplax. Activation by protons. *Journal of General Physiology* **82**, 25–42.

Hille, B. (1992). *Ionic channels of excitable membranes.* Sinauer, Sunderland.

Jentsch, T. J., Günther, W., Pusch, M. & Schwappach, B. (1995). Properties of voltage-gated chloride channels of the ClC gene family. *Journal of Physiology* **482.P**, 19–25*S*.

Jentsch, T. J., Steinmeyer, K. & Schwarz, G. (1990). Primary structure of *Torpedo marmorata* chloride channel isolated by expression cloning in *Xenopus* oocytes. *Nature* **348**, 510–514.

Kieferle, S., Fong, P., Bens, M., Vandewalle, A. & Jentsch, T. J. (1994). Two highly homologous members of the ClC chloride channel family in both rat and human kidney. *Proceedings of the National Academy of Sciences of the USA* **91**, 6943–6947.

Krieg, P. A. & Melton, D. A. (1984). Functional messenger RNAs are produced by SP6 *in vitro* transcription of cloned cDNAs. *Nucleic Acids Research* **12**, 7057–7070.

Ludewig, U., Pusch, M. & Jentsch, T. J. (1996). Two physically distinct pores in the dimeric ClC-0 channel. *Nature* **383**, 340–343.

Methfessel, C., Witzemann, V., Takahashi, T., Mishina, M., Numa, S. & Sakmann, B. (1986). Patch clamp measurements on *Xenopus laevis* oocytes: currents through endogenous channels and implanted acetylcholine receptor and sodium channels. *Pflügers Archiv* **407**, 577–588.

Middleton, R. E., Pheasant, D. J. & Miller, C. (1994). Purification reconstitution, and subunit composition of a voltage-gated chloride channel from *Torpedo* electroplax. *Biochemistry* **33**, 13189–13198.

Middleton, R. E., Pheasant, D. J. & Miller, C. (1996). Homodimeric structure of a ClC-type channel. *Nature* **383**, 337–340.

Miller, C. (1982). Open-state substructure of single chloride channels from *Torpedo* electroplax. *Philosophical Transactions of the Royal Society London* B **299**, 401–411.

Miller, C. & Richard, E. A. (1990). The voltage-dependent chloride channel of *Torpedo* electroplax. Intimations of molecular structure from quirks of single-channel function. In *Chloride Channels and Carriers in Nerve, Muscle, and Glial Cells*, ed. Alvarez-Leefmans F. J. & Russell, J. M., pp. 383–405. Plenum Press, New York.

Miller, C. & White, M. M. (1984). Dimeric structure of single chloride channels from *Torpedo* electroplax. *Proceedings of the National Academy of Sciences of the USA* **81**, 2772–2775.

Pusch, M., Ludewig, U., Rehfeldt, A. & Jentsch, T. J. (1995*a*). Gating of the voltage-dependent chloride channel ClC-0 by the permeant anion. *Nature* **373**, 527–531.

Pusch, M., Steinmeyer, K. & Jentsch, T. J. (1994). Low single channel conductace of the major skeletal muscle chloride channel, ClC-1. *Biophysical Journal* **66**, 149–152.

Pusch, M., Steinmeyer, K., Koch, M. C. & Jentsch, T. J. (1995*b*). Mutations in dominant human myotonia congenita drastically alter the voltage-dependence of the ClC-1 chloride channel. *Neuron* **15**, 1455–1463.

Rychkov, G. Y., Pusch, M., Astill, D. St J., Roberts, M. L., Jentsch, T. J. & Bretag, A. H. (1996). Concentration and pH dependence of skeletal muscle chloride channel ClC-1. *Journal of Physiology* (in the Press).

Sigworth, F. J. (1994). Voltage gating of ion channels. *Quarterly Reviews in Biophysics* **27**, 1–40.

Steinmeyer, K., Lorenz, C., Pusch, M., Koch, M. C. & Jentsch, T. J. (1994). Multimeric structure of ClC-1 chloride channels as revealed by mutations in dominant myotonia congenita (Thomsen). *EMBO Journal* **13**, 737–743.

Steinmeyer, K., Ortland, C. & Jentsch, T. J. (1991). Primary structure and functional expression of a developmentally regulated skeletal muscle chloride channel. *Nature* **354**, 301–304.

Stühmer, W. (1992). Electrophysiological recording from *Xenopus* oocytes. *Methods in Enzymology* **207**, 319–339.

THIEMANN, A., GRÜNDER, S., PUSCH, M. & JENTSCH, T. J. (1992). A chloride channel widely expressed in epithelial and non-epithelial cells. *Nature* **356**, 57–60.

UCHIDA, S., SASAKI, S., FURUKAWA, T., HIRAOKA, M., IWAI, T., HIRATA, Y. & MARUMO, F. (1993). Molecular cloning of a chloride channel that is regulated by dehydration and expressed predominantly in kidney medulla. *Journal of Biological Chemistry* **268**, 3821–3824.

WHITE, M. M. & MILLER, C. (1979). A voltage-gated anion channel from the electric organ of *Torpedo californica*. *Journal of Biological Chemistry* **254**, 10161–10166.

Acknowledgements

We thank Christine Neff for technical assistance and R. E. Middleton for discussion. This work was supported by grants of the Deutsche Forschungsgemeinschaft and the Fonds der Chemischen Industrie.

Note added in proof

Since this work was submitted for publication, T.-Y. Chen & C. Miller (*Journal of General Physiology* **108**, 237–250 (1996)) have published similar findings of the effect of internal chloride on the open probability of fast-gating channels, $P_{o,fast}$.

Author's email address

M. Pusch: pusch@uke.uni-hamburg.de

Received 20 June 1996; accepted 28 October 1996.